Supplementary Information

E2 enzyme inhibition by stabilization of a low affinity interface with ubiquitin

Hao Huang[1†], Derek F Ceccarelli[1†], Stephen Orlicky[1†], Daniel J. St-Cyr[2], Amy Ziemba[3], Pankaj Garg[4,5], Serge Plamondon[2], Manfred Auer[6], Sachdev Sidhu[4,5], Anne Marinier[2,7], Gary Kleiger[3], Mike Tyers[2,8*], Frank Sicheri[1,4*]

[1]Centre for Systems Biology, Samuel Lunenfeld Research Institute, Mount Sinai Hospital, Toronto, Canada M5G 1X5

[2] Institute for Research in Immunology and Cancer, University of Montreal, Montreal, Québec H3C 3J7, Canada

[3] Department of Chemistry, University of Nevada, Las Vegas, 4505 S. Maryland Parkway, Las Vegas, NV, 89154

[4]Department of Molecular Genetics, University of Toronto, Toronto, Ontario M5S 1A8, Canada

[5] Banting and Best Department of Medical Research, Terrence Donnelly Centre for Cellular and Biomolecular Research, University of Toronto, Toronto, Ontario M5S 3E1, Canada

[6]School of Biological Sciences, University of Edinburgh, Mayfield Road, Edinburgh EH9 3JR United Kingdom

[7]Department of Chemistry, University of Montreal, Montreal, Québec H3C 3J7, Canada

[8]Department of Medicine, University of Montreal, Montreal, Québec H3C 3J7, Canada

[†] these authors contributed equally to this work

[*]To whom correspondence should be addressed:

Frank Sicheri, sicheri@lunenfeld.ca, 416-586-8471

Mike Tyers, md.tyers@umontreal.ca, 514-343-6668

Supplementary Results

Supplementary Table 1. Data collection and refinement statistics for the CC0651-Cdc34A-ubiquitin complex. Data was collected from a single frozen crystal. Highest resolution shell is shown in parenthesis.

Data collection	
Space group	P1
Cell dimensions	
a, *b*, *c* (Å)	55.4, 72.2, 75.9
α, β, γ (°)	71.9, 79.6, 81.6
Resolution (Å)	44.6-2.6
R_{sym} or R_{merge}	7.9 (45.7)
$I/\sigma I$	13.7 (1.2)
Completeness (%)	95.8 (85.5)
Redundancy	2.2 (1.7)
Refinement	
Resolution (Å)	44.6-2.6
No. reflections	31377
$R_{work/}$ R_{free}	0.204/0.259
No. atoms	
Protein	7545
Ligand/ion	166
Water	46
B-factors	
Protein	39.2
Ligand/ion	56.9
Water	51.5
RMS deviations	
Bond lengths (Å)	0.008
Bond angles (º)	1.26

Supplementary Table 2. Compound Characterization Data

Compound	Analytical Data
1 (CC0651)	^{1}H NMR (400 MHz, CD_3OD): δ (ppm) 7.49-7.59 (m, 4H), 7.30-7.42 (m, 3 H), 4.37 (ddd, *J* = 9.8, 8.2, 4.3 Hz, 1 H), 4.30 (d, *J* = 2.0 Hz, 1 H), 3.99 (dd, *J* = 8.2, 2.0 Hz, 1 H), 3.81 (d, *J* = 15.3 Hz, 1 H), 3.71 (d, *J* = 15.3 Hz, 1 H), 3.3 (s, 3 H, overlapping with solvent), 3.24 (dd, *J* = 14.1, 4.3 Hz, 1 H), 2.87 (dd, *J* = 13.9, 10.0 Hz, 1 H). LC (Method B): Ret. time = 2.14 min. HRMS (ESI-TOF) *m*/*z*: $[M + H]^+$ Calcd for $C_{20}H_{22}Cl_2NO_6$ 442.0819; found: 442.0813. $[\alpha]_D^{20}$ 41 (*c* 0.18, $CHCl_3$).
2	^{1}H NMR (400 MHz, CD_3OD): δ (ppm) 7.49 (pseudo d, *J* = 8.1 Hz, 2 H), 7.31 (pseudo d, *J* = 8.2 Hz, 2 H), 7.18 (s, 2H), 6.96 (s, 1 H), 4.41-4.33 (m, 1 H, C*H*N), 4.31 (d, *J* = 1.8 Hz, 1H, C*H*CO_2H), 3.98 (dd, *J* = 7.9, 1.8 Hz, 1 H, OC*H*CHN), 3.83 (d, *J* = 15.3 Hz, 1 H, C*H*$_2$OMe), 3.72 (d, *J* = 15.3 Hz, 1 H, C*H*$_2$OMe), 3.30 (s, 3 H, OC*H*$_3$, overlapping with solvent signal), 3.21 (dd, *J* = 13.9, 4.5 Hz, 1 H, C*H*$_2$Ar), 2.86 (dd, *J* = 14.1, 9.7 Hz, 1 H. C*H*$_2$Ar), 2.34 (s, 6 H, ArC*H*$_3$). ^{13}C NMR (100 MHz, CD_3OD, $CH_{(1-3)}$ from HSQC): δ (ppm) 130.6 (CH), 129.4 (CH), 127.7 (CH), 125.5 (CH), 74.0 (O*C*HCN), 72.3 (C*H*$_2$OMe), 71.9 (*C*HCO2H), 59.3 (O*C*H_3), 53.9 (*C*HN), 37.3 (CH_2), 21.2 (CH_3). HRMS (ESI-TOF) *m*/*z*: $[M + H]^+$ Calcd for $C_{22}H_{28}NO_6$ 402.1911; Found 402.1934.
3	^{1}H NMR (400 MHz , CD_3OD): δ (ppm) 7.60-7.51 (m, 2 H), 7.42-7.32 (m, 2 H), 7.28-7.15 (m, 2 H), 6.93-6.84 (m, 1 H), 4.43-4.33 (m, 1 H), 4.23 (d, *J* = 1.9 Hz, 1 H), 3.97 (dd, *J* = 7.9, 1.9 Hz, 1 H), 3.81 (d, *J* = 15.6 Hz, 1 H), 3.71 (d, *J* = 15.3 Hz, 1 H), 3.30 (s, 3 H, overlapping with solvent signal), 3.23 (dd, *J* = 13.8, 4.4 Hz, 1 H), 2.86 (dd, *J* = 13.9, 9.8 Hz, 1 H). ^{13}C NMR (100 MHz, CD_3OD, $CH_{(1-3)}$ from HSQC): δ (ppm) 131.0 (CH), 127.7 (CH), 110.3 (CH), 102.7 (CH), 74.0 (O*C*HCN), 72.3 (C*H*$_2$OMe), 72.1 (*C*HCO2H), 59.3 (O*C*H_3), 53.9 (*C*HN), 37.5 (CH_2Ar). HRMS (ESI-TOF) *m*/*z*: $[M + H]^+$ Calcd for $C_{20}H_{22}F_2NO_6$ 410.1410; Found 410.1420.
4	^{1}H NMR (400MHz ,cd_3od): δ (ppm) 7.50 (pseudo d, *J* = 8.2 Hz, 2 H), 7.35 (s, 1 H), 7.33-7.26 (m, 3 H), 7.16 (d, *J* = 7.9 Hz, 1 H), 4.41-4.32 (m, 1 H), 4.31-4.26 (m, 1 H), 3.98 (d, *J* = 8.2 Hz, 1 H), 3.82 (d, *J* = 15.3 Hz, 1 H), 3.72 (d, *J* = 15.3 Hz, 1 H), 3.30 (s, 3 H, overlapping with solvent signal), 3.20 (dd, *J* = 14.1, 4.4 Hz, 1 H), 2.85 (dd, *J* = 13.8, 9.7 Hz, 1 H), 2.31 (s, 3 H), 2.28 (s, 3

	H). ^{13}C NMR (100 MHz, CD_3OD, $CH_{(1-3)}$ from HSQC): δ (ppm) 130.8 (CH), 130.5 (CH), 128.7 (CH), 127.4 (CH), 124.9 (CH), 73.9 (CH), 72.3 (CH_2), 72.0 (CH), 59.3 (CH_3), 53.9 (CH), 37.3 (CH_2), 19.7 (CH_3), 19.2 (CH_3). HRMS (ESI-TOF) *m*/*z*: $[M + H]^+$ Calcd for $C_{22}H_{28}NO_6$ 402.1911; found 402.1926.
5	^{1}H NMR (400 MHz , CD_3OD): δ (ppm) 7.52 (psudo d, *J* = 8.2 Hz, 2 H), 7.32 (pseudo d, *J* = 8.2 Hz, 2 H), 6.93-6.79 (m, 2 H), 4.42-4.34 (m, 1 H), 4.27 (d, *J* = 1.5 Hz, 1 H), 3.97 (dd, *J* = 7.6, 1.4 Hz, 1 H), 3.90 (s, 6 H), 3.83 (d, *J* = 15.1 Hz, 1 H), 3.79 (s, 3 H), 3.73 (d, *J* = 15.3 Hz, 1 H), 3.32 (s, 3 H, overlapping with solvent signal), 3.21 (dd, *J* = 13.9, 4.3 Hz, 1 H), 2.86 (dd, *J* = 13.9, 9.5, 1 H). ^{13}C NMR (100 MHz, CD_3OD, $CH_{(1-3)}$ from HSQC): δ (ppm) 130.1 (CH), 127.2 (CH), 104.7 (Ar *C*HCO), 73.7 (O*C*HCN), 71.9 (C*H*$_2$OMe), 71.5 (*C*HCO2H), 60.8 (*p*-ArO*C*H$_3$), 58.9 (CH_2O*C*H$_3$), 56.0 (*m*-ArO*C*H$_3$), 53.7 (*C*HN), 36.8 (*C*H$_2$Ar). HRMS (ESI-TOF) *m*/*z*: $[M + H]^+$ Calcd for $C_{23}H_{30}NO_9$ 464.1915; found 464.1926.
6	^{1}H NMR (400MHz , CD_3OD): δ (ppm) 7.51 (d, *J* = 8.2 Hz, 2 H), 7.46 (d, *J* = 7.3 Hz, 2 H), 7.41-7.35 (m, 2 H), 7.35-7.27 (m, 4 H), 7.21-7.14 (m, 2 H), 6.96 (dd, *J* = 2.1, 7.9 Hz, 1 H), 5.14 (s, 2 H), 4.37 (d, *J* = 2.9 Hz, 1 H), 4.32-4.24 (m, 1 H), 3.98 (d, *J* = 8.2 Hz, 1 H), 3.82 (d, *J* = 15.3 Hz, 1 H), 3.72 (d, *J* = 15.3 Hz, 1 H), 3.30 (s, 3 H, overlapping with solvent signal), 3.21 (dd, *J* = 4.4, 13.8 Hz, 1 H), 2.86 (dd, *J* = 9.8, 13.9 Hz, 1 H). ^{13}C NMR (100 MHz, CD_3OD, $CH_{(1-3)}$ from HSQC): δ (ppm) 130.6 (CH), 129.3 (CH), 128.7 (CH), 128.3 (CH), 127.6 (CH), 120.2 (CH), 114.4 (CH), 114.3 (CH), 73.9 (O*C*HCN), 72.3 (C*H*$_2$OMe), 71.9 (*C*HCO2H), 70.8 (O*C*H$_2$Ar), 59.1 (CH_2O*C*H$_3$), 54.0 (*C*HN), 37.2 (*C*H$_2$Ar). HRMS (ESI-TOF) *m*/*z*: $[M + H]^+$ Calcd for $C_{27}H_{30}NO_7$ 480.2017; found 480.2044.
7	^{1}H NMR (400 MHz, $CDCl_3$): δ (ppm) 7.43 (pseudo d, *J* = 8.6 Hz, 2 H), 7.10 (pseudo d, *J* = 8.2 Hz, 2 H), 4.72 (br. s., 1 H), 3.83 (br. s., 1 H), 3.61-3.72 (m, 1 H), 3.48-3.61 (m, 1 H), 2.81 (d, *J* = 7.04 Hz, 2 H), 2.19 (br. s., 1 H), 1.42 (s, 9 H). LC (Method A): Ret. time = 2.22 min. LC-MS (APCI) *m*/*z*: [M - Boc + H_2]$^+$ Calcd for $C_9H_{13}BrNO$ 230.0; found 230.2, 232.0. $[\alpha]_D^{20}$ –24.9 (*c* 1.07, $CHCl_3$).
8	^{1}H NMR (400 MHz, $CDCl_3$): δ (ppm) 7.49 (d, *J* = 8.2 Hz, 2 H), 7.41-7.46 (m, 2 H), 7.28-7.36 (m, 3 H), 4.76 (br. s., 1 H), 3.91 (br. s., 1 H), 3.71 (dt, *J* =

	10.3, 4.8 Hz, 1 H), 3.60 (dt, *J* = 10.8, 5.2 Hz, 1 H), 2.91 (d, *J* = 7.0 Hz, 2 H), 2.19 (br. s., 1 H), 1.43 (s, 9 H). LC (Method A): Ret. time = 2.69 min. LC-MS (APCI) *m*/*z*: $[M - Boc + H_2]^+$ Calcd for $C_{15}H_{16}Cl_2NO$ 296.1; found 296.0, 298.2.
9	^1H NMR (400 MHz, $CDCl_3$): δ (ppm) 9.67 (s, 1 H), 7.49 (d, *J* = 7.0 Hz, 2 H), 7.44 (s, 2 H), 7.34 (d, *J* = 1.6 Hz, 1 H), 7.27 (t, *J* = 3.5 Hz, 3 H), 5.08 (br. s., 1 H), 4.48 (d, *J* = 5.9 Hz, 1 H), 3.03-3.32 (m, 2 H), 1.45 (s, 9 H).
10	^1H NMR (400 MHz, $CDCl_3$): δ (ppm) 7.49 (d, *J* = 8.2 Hz, 2 H), 7.45 (d, *J* = 2.0 Hz, 2 H), 7.32-7.37 (m, 1 H), 7.23-7.30 (m, 2 H), 6.93 (dd, *J* = 15.7, 5.1 Hz, 1 H), 5.82-5.96 (m, 1 H), 4.65 (br. s., 1 H), 4.54 (br. s., 1 H), 3.74 (s, 3 H), 2.95 (d, *J* = 6.7 Hz, 2 H), 1.31-1.49 (m, 9 H). LC (Method A): Ret. time = 2.89 min. LC-MS (APCI) *m*/*z*: $[M - Boc + H_2]^+$ Calcd for $C_{18}H_{18}Cl_2NO_2$ 350.1; found 350.2, 352.0.
11	^1H NMR (400 MHz, CD_3OD): δ (ppm) 7.48-7.60 (m, 4 H), 7.32-7.43 (m, 3 H), 4.31-4.40 (m, 1 H), 3.93 (td, *J* = 9.5, 3.7 Hz, 1 H), 3.69-3.88 (m, 4 H), 3.24 (dd, *J* = 13.7, 3.5 Hz, 1 H), 2.70 (dd, *J* = 13.7, 10.2 Hz, 1 H), 1.26-1.38 (m, 9 H). LC (Method A): Ret. time = 2.79 min. LC-MS (APCI) *m*/*z*: $[M - Boc + H_2]^+$ Calcd for $C_{18}H_{20}Cl_2NO_4$ 384.1; found 384.0, 386.0.
12	^1H NMR (400 MHz, CD_3OD): δ (ppm) 7.50-7.60 (m, 4 H), 7.33-7.43 (m, 3 H), 4.32-4.42 (m, 2 H), 3.97 (dd, *J* = 8.0, 2.2 Hz, 1 H), 3.68-3.86 (m, 5 H), 3.33 (s, 3 H, overlapping with solvent signal), 3.23 (dd, *J* = 13.7, 4.3 Hz, 1 H), 2.87 (dd, *J* = 13.9, 10.0 Hz, 1H). LC (Method A): Ret. time = 2.22 min. LC-MS (APCI) *m*/*z*: $[M + H]^+$ Calcd for $C_{21}H_{24}Cl_2NO_6$ 456.1; found 456.2, 458.0.

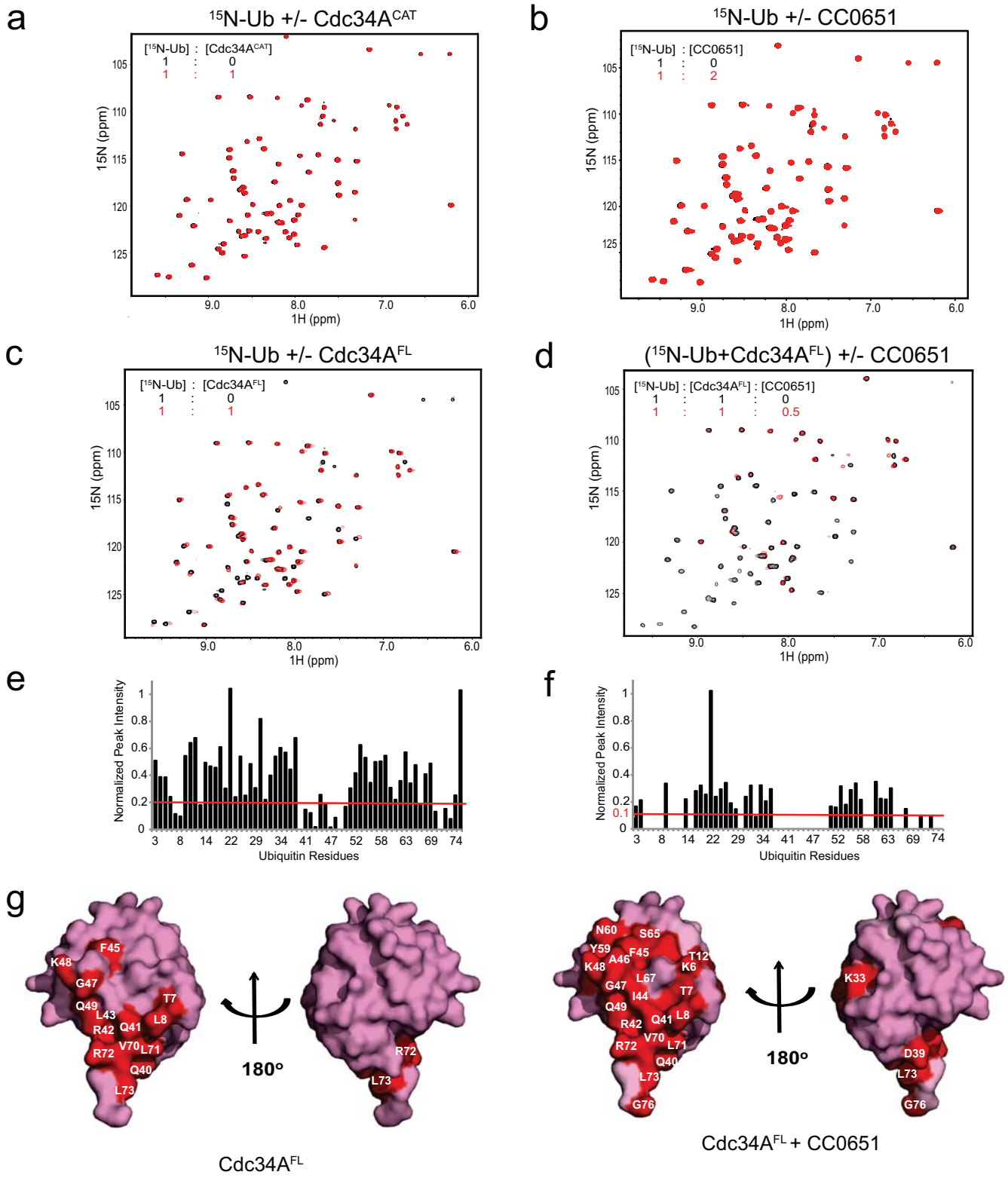

Supplementary Figure 1. Interaction analysis of ^{15}N-Ub, Cdc34A and CC0651. (a-d) Superposition of the ^{1}H, ^{15}N-HSQC spectra of (a) ^{15}N-Ub (black) versus ^{15}N-Ub:Cdc34A^{CAT} (red), (b) ^{15}N-Ub (black) versus ^{15}N-Ub:CC0651 (red), (c) ^{15}N-Ub (black) versus ^{15}N-Ub:Cdc34A^{FL} (red) and (d) ^{15}N-Ub:Cdc34A^{FL} (black) versus ^{15}N-Ub:Cdc34A^{FL}:CC0651 (red). Stoichiometric ratios of components in each experiment are indicated. (e-f) Peak intensity change versus residue number for (e) ^{15}N-Ub versus ^{15}N-Ub:Cdc34A^{FL} (panel c) and (f) ^{15}N-Ub:Cdc34A^{FL} versus ^{15}N-Ub:Cdc34A^{FL}:CC0651 (panel d). (g) Interaction surfaces on ubiquitin for Cdc34A^{FL} in the absence and presence of CC0651. Surfaces were defined using peak intensity change cut-offs shown as red dashed lines in panels e and f.

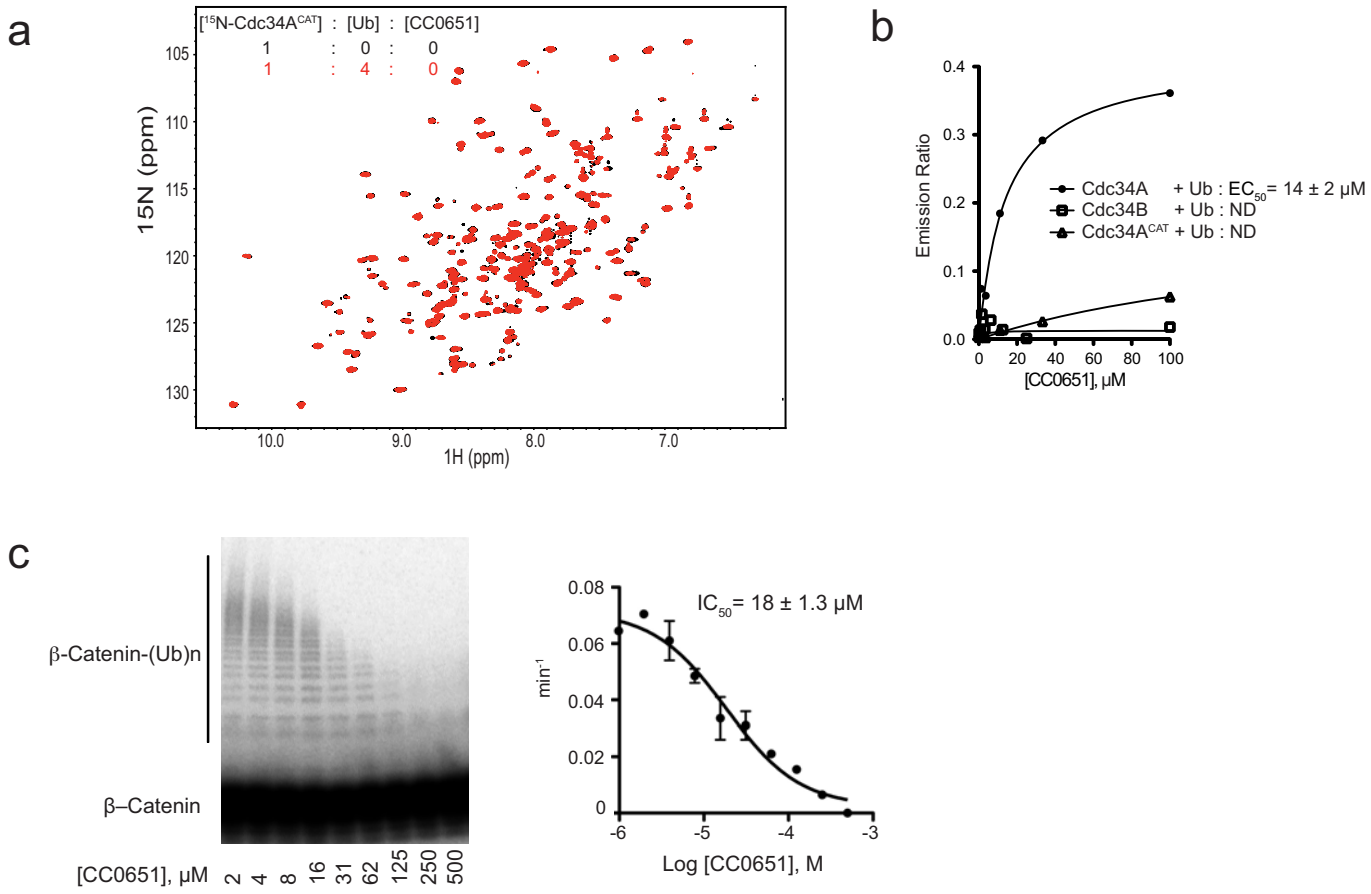

Supplementary Figure 2. CC0651 potentiates the interaction between ^{15}N-Cdc34A and ubiquitin. (a) Superposition of ^{1}H, ^{15}N-HSQC spectra at the indicated molar ratios for ^{15}N-Cdc34A^{CAT} (black) versus ^{15}N-Cdc34A^{CAT}:Ub (red). (b) CC0651 titration analysis of indicated E2 enzyme binding to ubiquitin using a TR-FRET assay. Data presented as mean +/- S.E.M., n=2. (c) Dose response inhibition profile of CC0651 on the ubiquitination of β-catenin peptide substrate by SCF β-TrCP. Fluorescence intensities of polyubiquitin signals were quantified and plotted as mean +/- S.E.M., n=2.

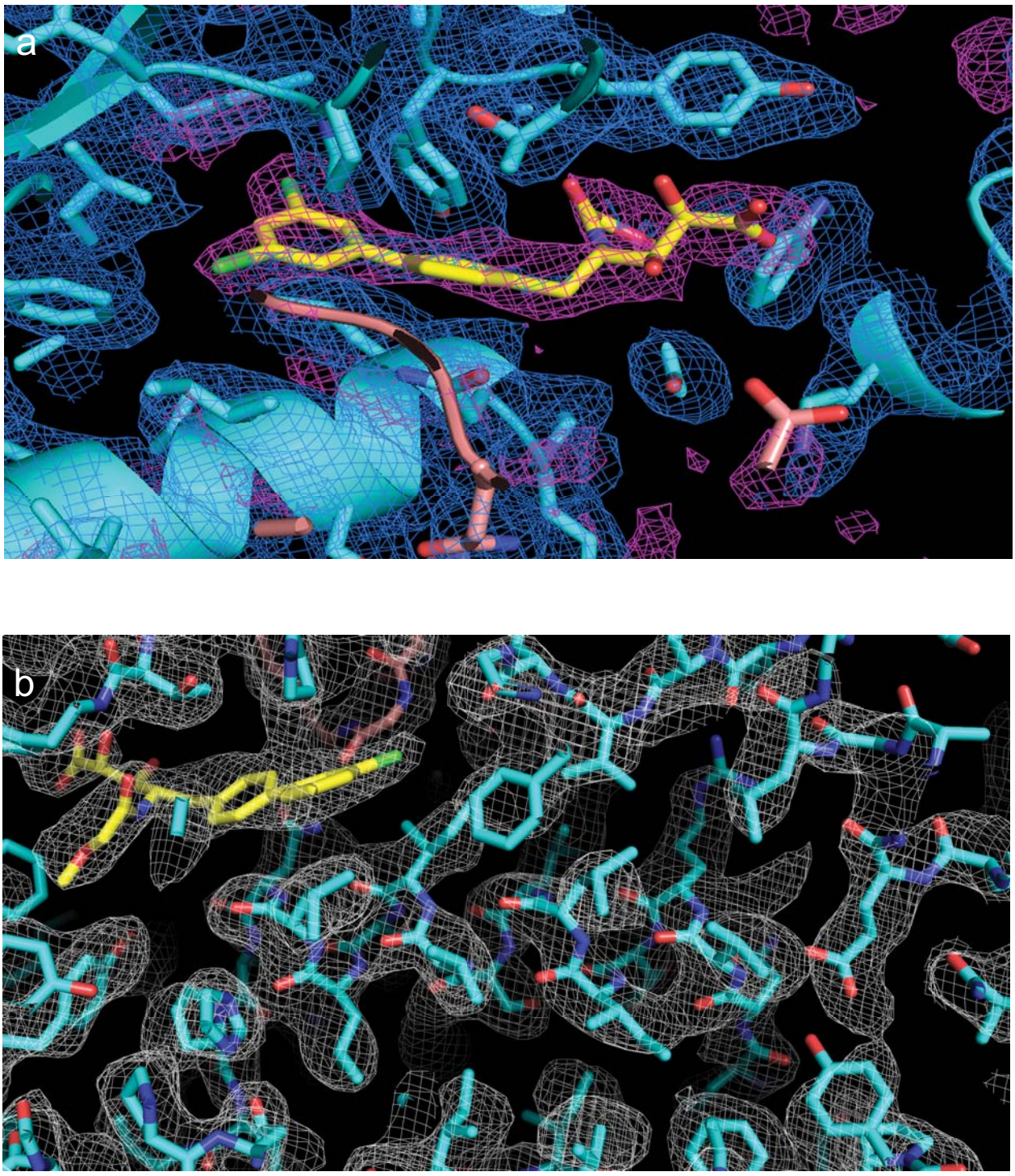

Supplementary Figure 3. Representative electron density maps. (a) Unbiased electron density map of the CC0651-Cdc34A-ubiquitin complex before inclusion of CC0651 coordinates into the refinement model. 2Fo-Fc map in blue (contoured at 1.0σ) and Fo-Fc map in magenta (contoured at 2.5σ) are centered on the CC0651 binding pocket. CC0651, Cdc34A and ubiquitin are colored yellow, cyan and pink respectively. (b) Prime-and-switch generated electron density map of the CC0651-Cdc34A-ubiquitin complex contoured at 1.0σ. Coloring as in (a).

a

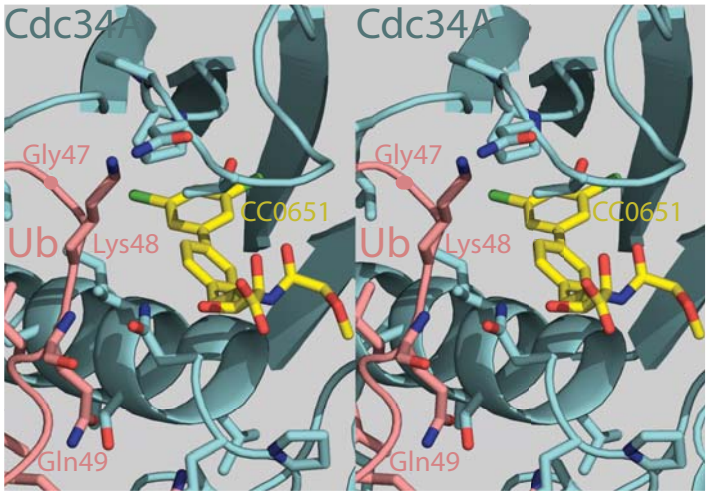

b

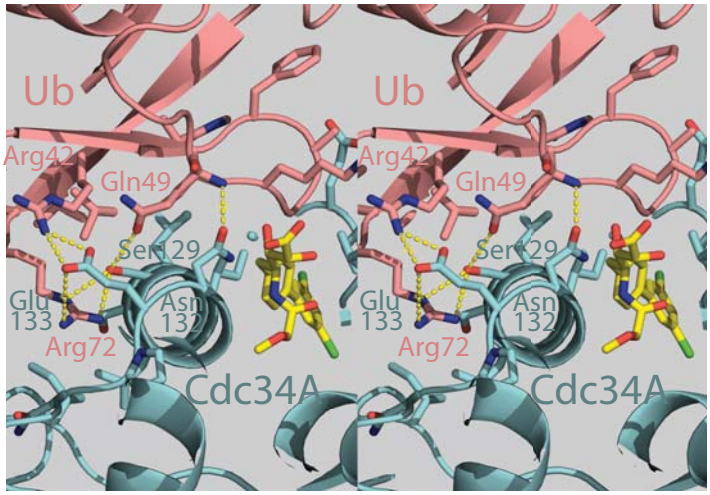

c

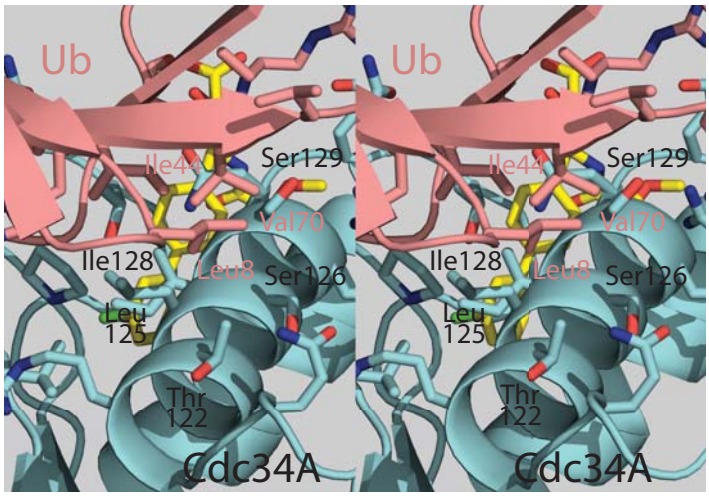

Supplementary Figure 4. Notable contact features of the CC0651-Cdc34A-ubiquitin complex. Stereo views are shown for (a) contacts between ubiquitin and CC0651, (b) hydrogen bonding network between ubiquitin and Cdc34A and (c) hydrophobic contacts between ubiquitin and Cdc34A. Color scheme as in Fig. 3.

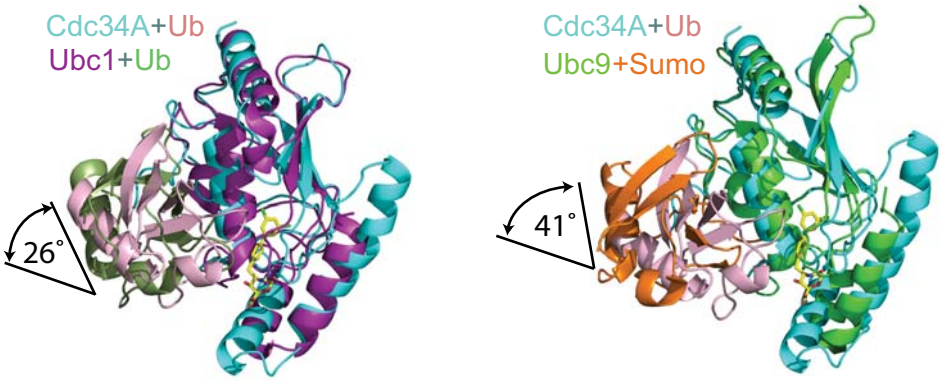

Supplementary Figure 5. Binding orientation of ubiquitin to Cdc34A induced by CC0651 is similar to a previously characterized E2-SUMO interaction. Overlay of the CC0651-Cdc34A-ubiquitin complex with a UbcH9-SUMO complex (PDB 1Z5S [1]) is shown. Superposition was performed using the E2 coordinates. Rotation angles relate the orientations of ubiquitin and SUMO subunits. Overlay of the CC0651-Cdc34A-ubiquitin complex with the Ubc1-Ub covalent complex (PDB 1FXT [2]) shown in Fig. 3e is included for reference.

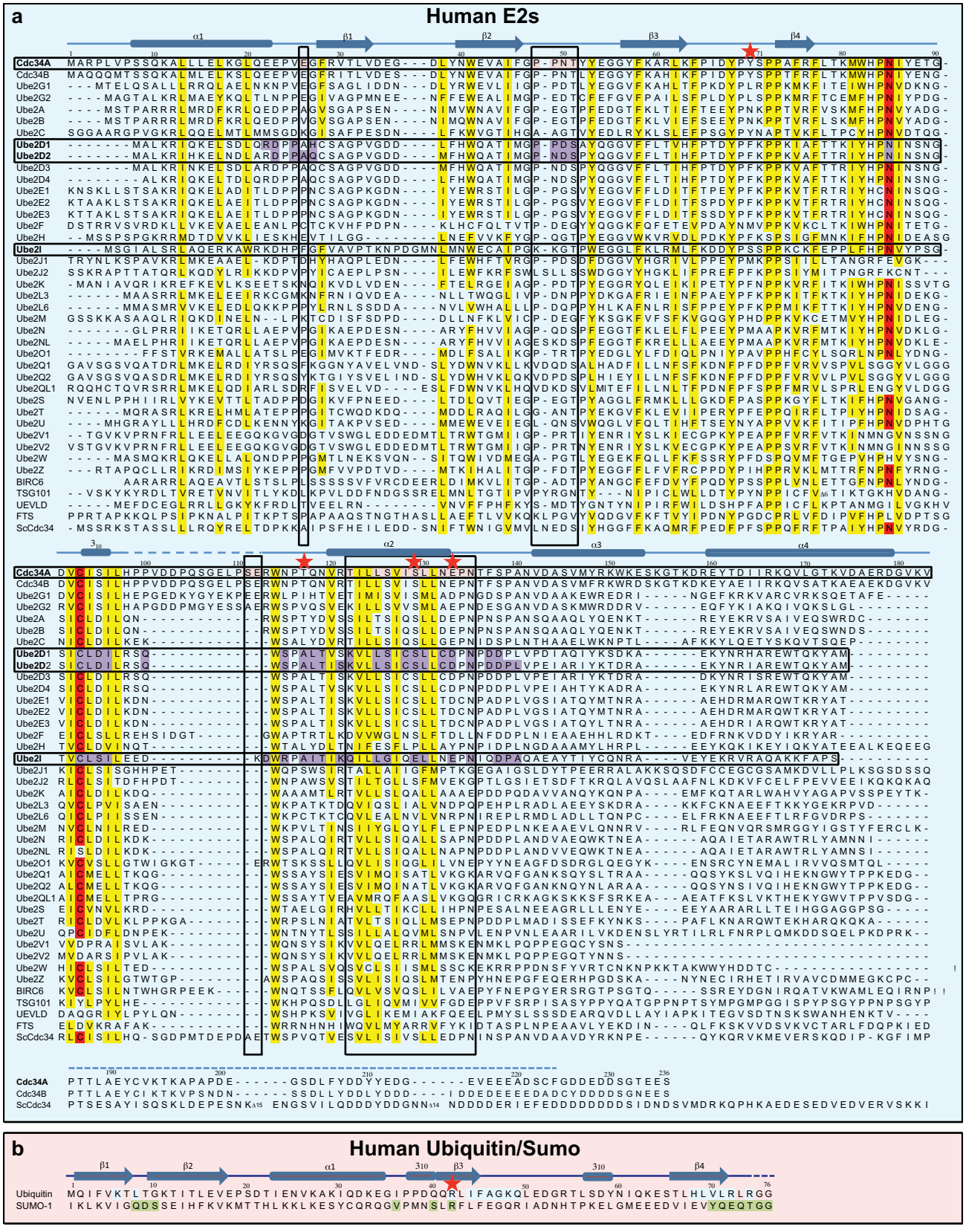

Supplementary Figure 6. Structure-based sequence alignments for human E2 enzymes and for ubiquitin. (a) Residue numbers and secondary structure elements for human Cdc34A are indicated above the aligned sequences. A region of disorder in the Cdc34A structure is indicated by a dashed line. Residues mutated in this study are highlighted by red stars. The catalytic cysteine and asparagine are in red and conserved hydrophobic residues in yellow. Cdc34A residues comprising the ubiquitin interface are in pink and boxed across all E2 enzymes. Cdc34A ubiquitin contact residues of UbcH5A and UbcH5B (PDB 4AP4; PDB 4AUQ), and Ubc9 (PDB 1Z5S) are in purple. (b) Residue numbers and secondary structure elements for human ubiquitin are indicated above the aligned sequences of wild type ubiquitin and SUMO-1. Residues that contact Cdc34A and Ubc9 are in cyan and green.

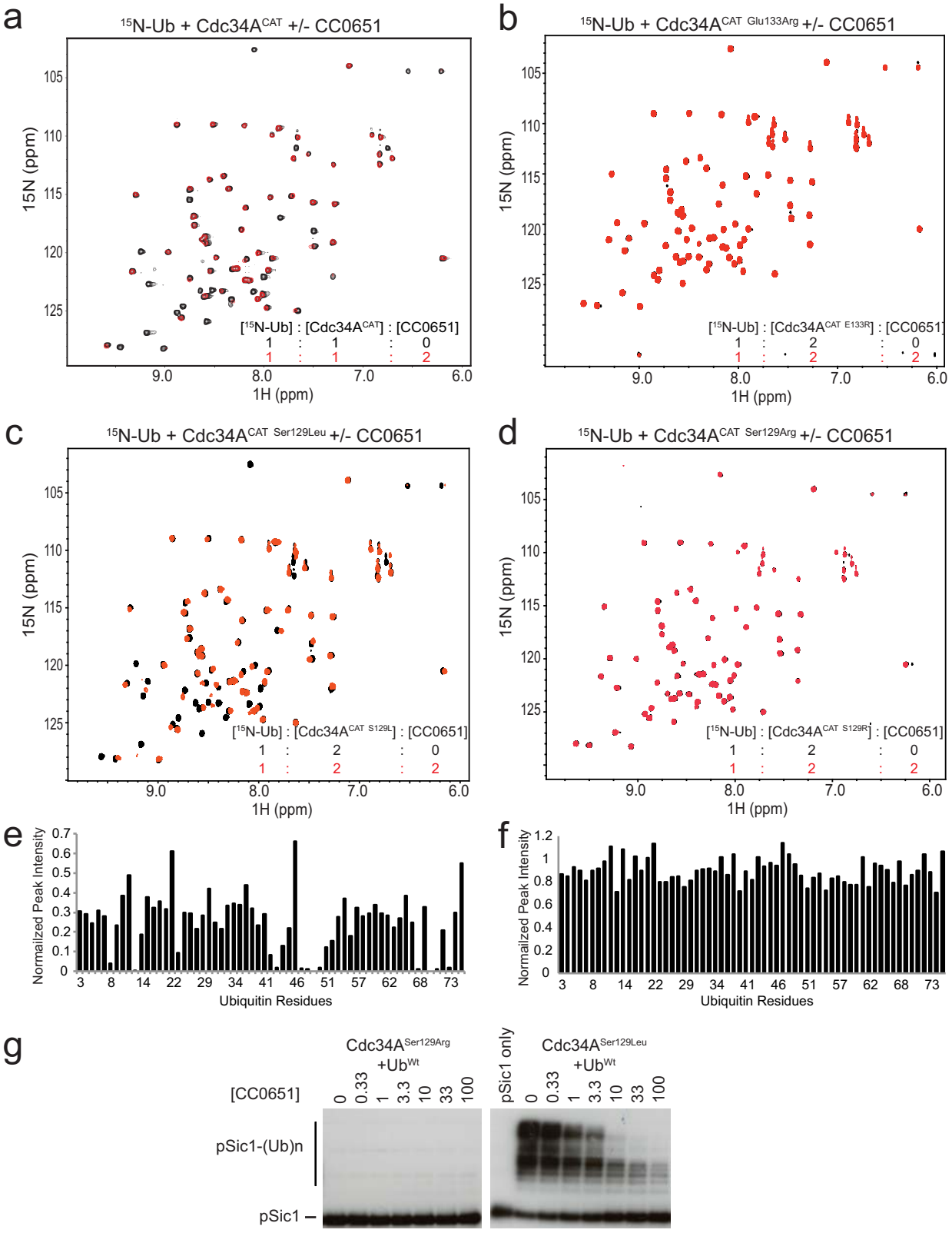

Supplementary Figure 7. Effect of structure-guided mutations in Cdc34A on interactions of ^{15}N-Ub, Cdc34A and CC0651 detected by NMR. (a-d) Superposition of the ^{1}H, ^{15}N-HSQC spectra of (a) ^{15}N-Ub:Cdc34A^{CAT} (black) versus ^{15}N-Ub:Cdc34A^{CAT}:CC0651 (red), (b) ^{15}N-Ub:Cdc34A$^{CAT\text{-}Glu133Arg}$ (black) versus ^{15}N-Ub:Cdc34A$^{CAT\text{-}Glu133Arg}$:CC0651 (red), (c) ^{15}N-Ub:Cdc34A$^{CAT\text{-}Ser129Leu}$ (black) versus ^{15}N-Ub:Cdc34A$^{CAT\text{-}Ser129Leu}$:CC0651 (red) and (d) ^{15}N-Ub:Cdc34A$^{CAT\text{-}Ser129Arg}$ (black) versus ^{15}N-Ub:Cdc34$^{CAT\text{-}Ser129Arg}$:CC0651 (red). Stoichiometric ratios of each component are indicated. (e-f) Peak intensity change versus residue number for the ^{1}H, ^{15}N-HSQC spectra of (e) ^{15}N-ubiquitin:Cdc34A$^{CAT\ Ser129Leu}$ versus ^{15}N-ubiquitin:Cdc34A$^{CAT\ Ser129Leu}$:CC0651 (panel c) and (f) ^{15}N-ubiquitin:Cdc34A$^{CAT\ Ser129Arg}$ versus ^{15}N-ubiquitin:Cdc34A$^{CAT\ Ser129Arg}$:CC0651 (panel d). (g) Sensitivity of the SCF^{Cdc4} Sic1 ubiquitination reaction to CC0651 for the indicated mutants of Cdc34A.

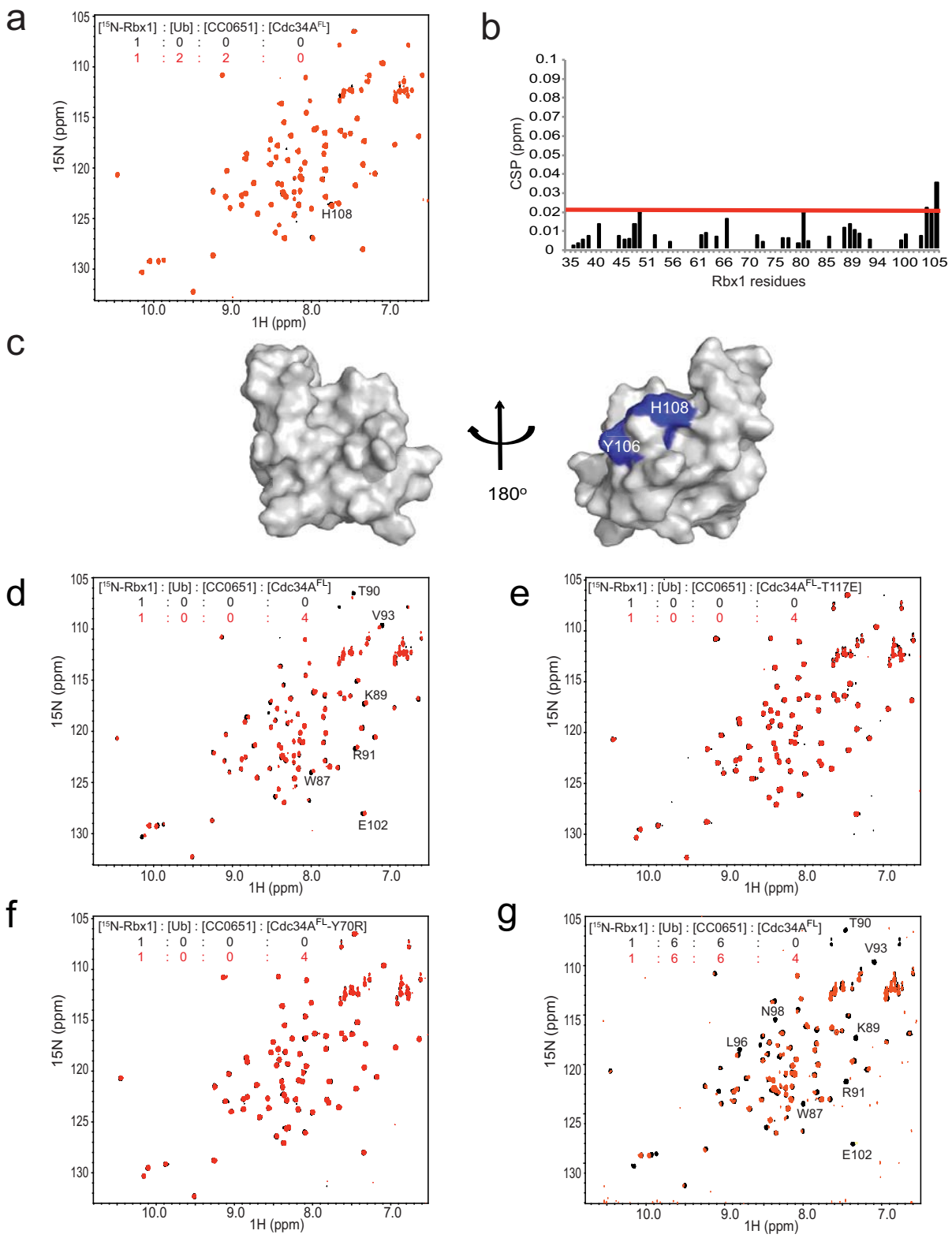

Supplementary Figure 8. Interaction analysis of ^{15}N-Rbx1 with Cdc34A, ubiquitin and CC0651. (a) Superposition of the ^{1}H, ^{15}N-HSQC spectra of ^{15}N-Rbx1 (residues 12-108) (black) versus ^{15}N-Rbx1 (residues 12-108):Ub:CC0651 (red) are shown for the indicated stoichiometric ratios. (b) Chemical shift perturbation for the ^{1}H, ^{15}N-HSQC spectra superpositions in panel a. (c) Front and back surface representations of the Rbx1 RING domain (PDB 2LGV [3]) with residues affected by the addition of ubiquitin and CC0651 to ^{15}N-Rbx1 shown in blue. Affected residues were defined by the red line in panel b. (d-g) Superposition of ^{1}H, ^{15}N-HSQC spectra for (d) ^{15}N-Rbx1 (black) versus ^{15}N-Rbx1:Cdc34A^{FL} (red), (e) ^{15}N-Rbx1 (black) versus ^{15}N-Rbx1:Cdc34A$^{FL\text{-}Thr117Glu}$ (red), (f) ^{15}N-Rbx1 (black) versus ^{15}N-Rbx1:Cdc34A$^{FL\text{-}Tyr70Arg}$ (red), and (g) ^{15}N-Rbx1:CC0651:ubiquitin (black) versus ^{15}N Rbx1:CC0651:Cdc34A^{FL}:ubiquitin (red) at the indicated stoichiometric ratios.

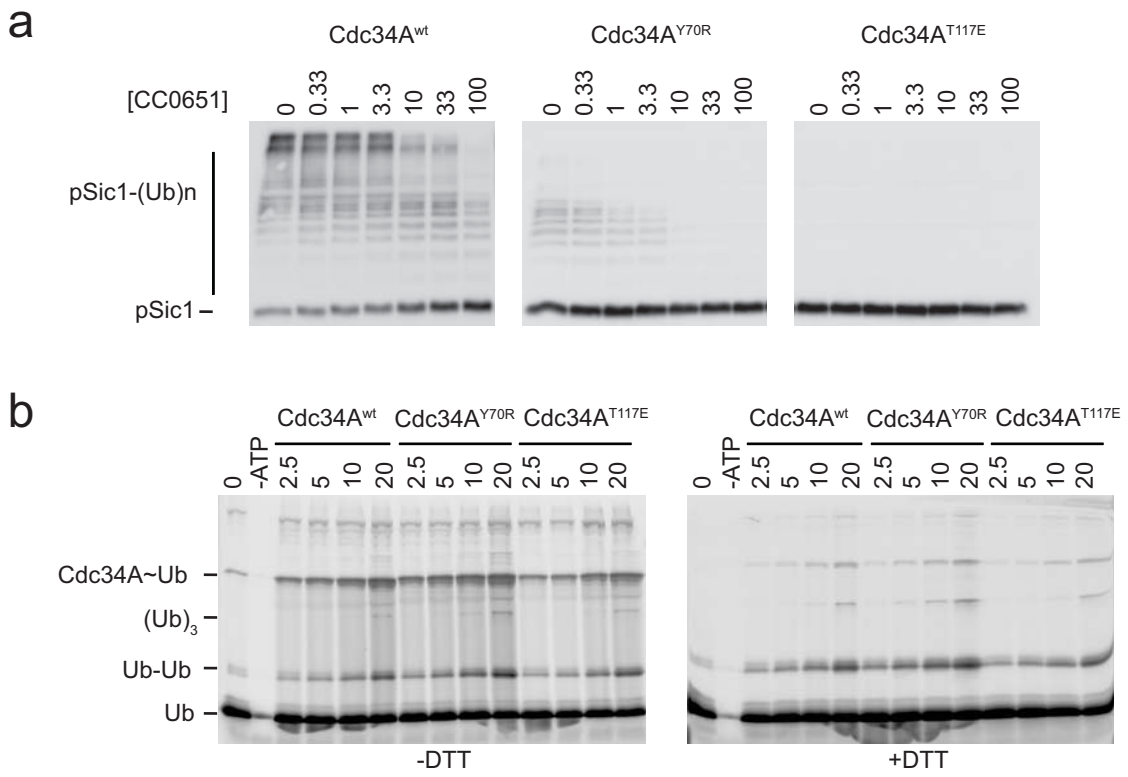

Supplementary Figure 9. Functional characterization of Cdc34A mutations that alter the Rbx1 interaction. (a) Sensitivity of the SCF^{Cdc4} Sic1 ubiquitination reaction to CC0651 for wild type, Tyr70Arg and Thr117Glu versions of Cdc34A. (b) Charging of wild type, Tyr70Arg and Thr117Glu versions of Cdc34A by E1 enzyme. Cdc34A-ubiquitin thioester was detected under non-reducing conditions (-DTT).

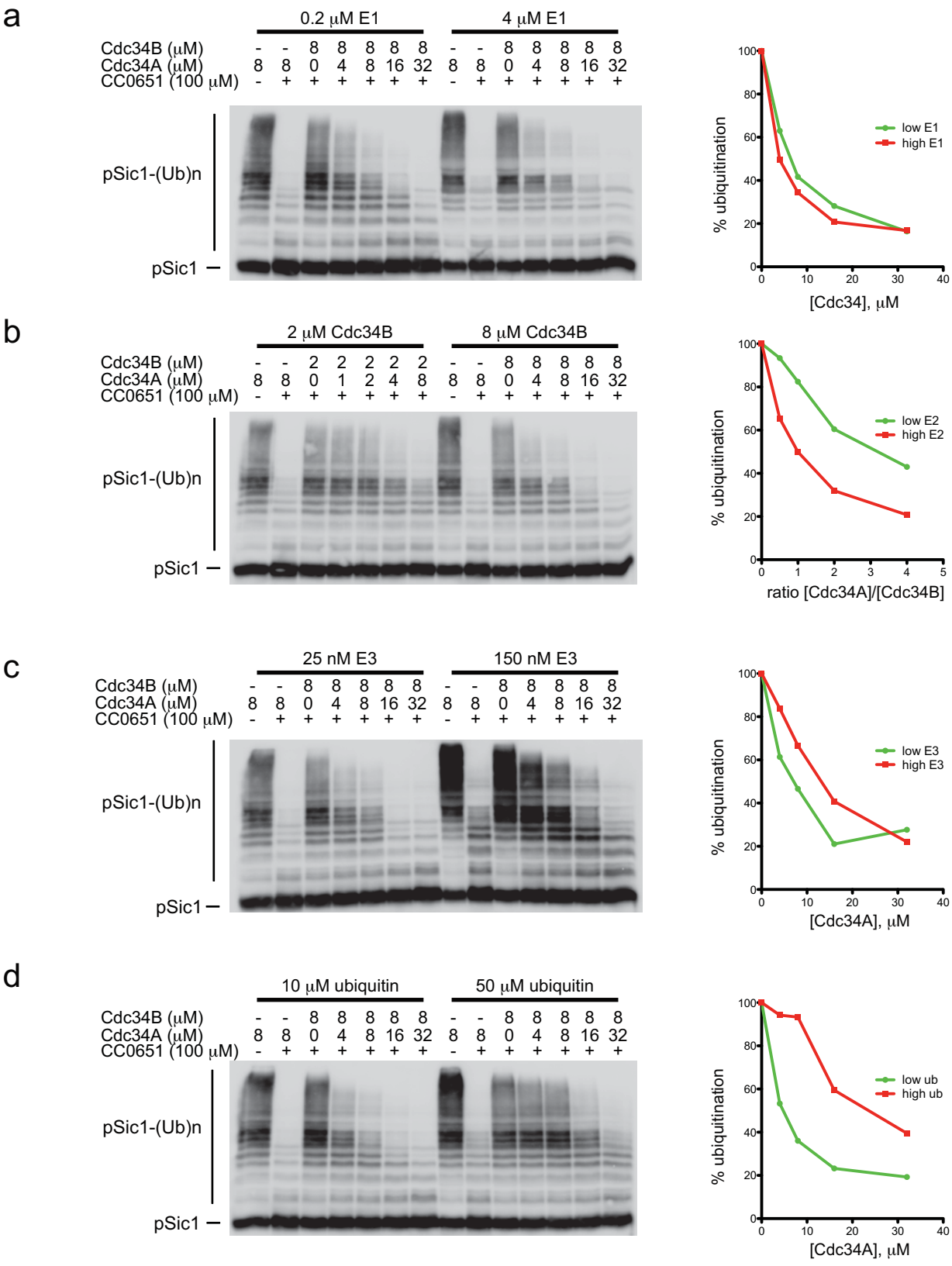

Supplementary Figure 10. Dominant interference of the CC0651-Cdc34A-ubiquitin complex on Cdc34B-SCF^{Cdc4} activity. The CC0651-Cdc34A complex was titrated into Sic1 ubiquitination reactions in the presence of a fixed concentration of Cdc34B in the presence of the indicated concentrations of E1, E2, E3 and ubiquitin, in the presence or absence of 100μM CC0651. Concentrations of Cdc34A and Cdc34B are in μM.

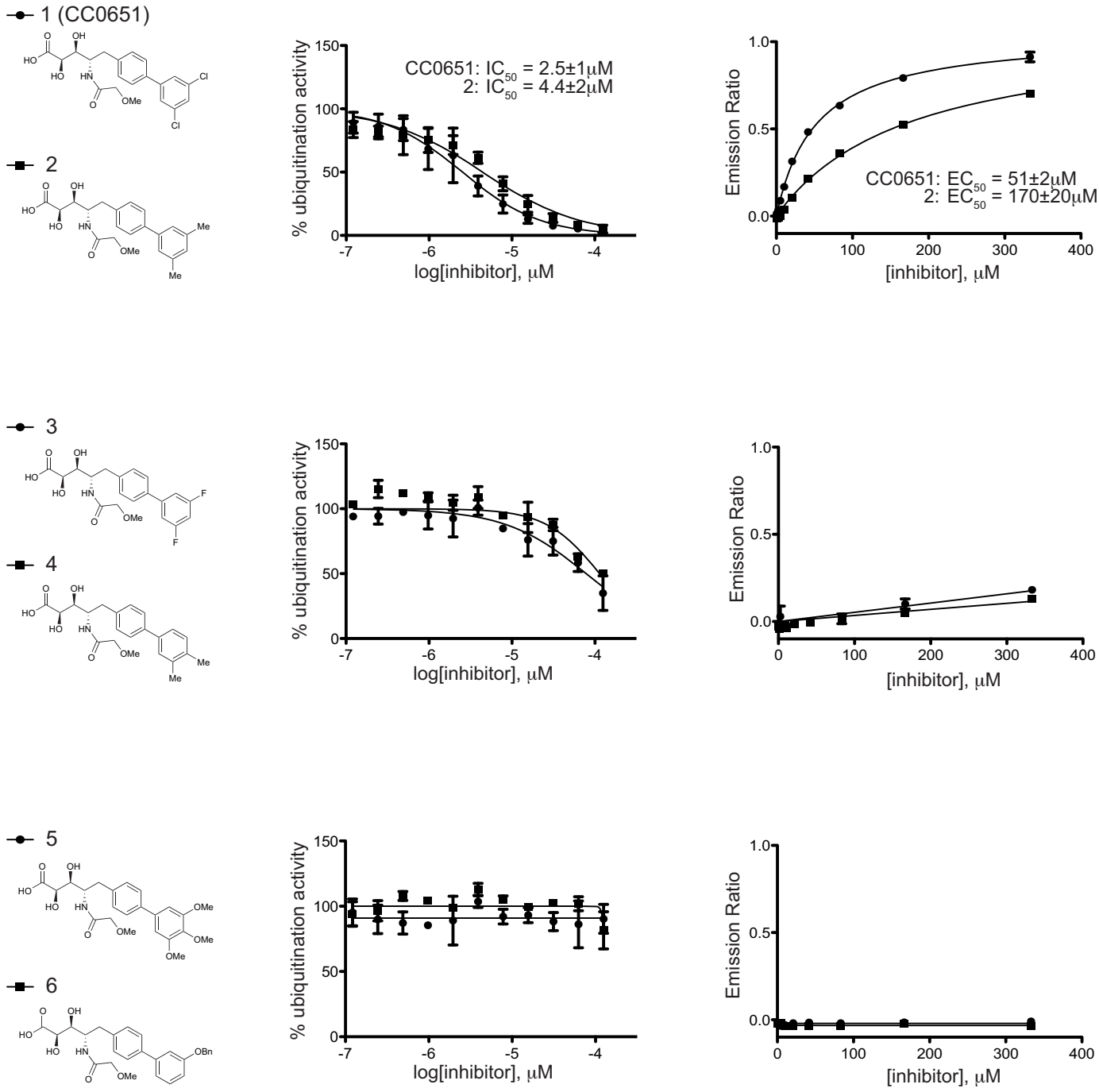

Supplementary Figure 11. CC0651 structure-activity relationship analysis. (left) Structure of CC0651 analogs. Benzyl moiety is indicated by Bn. (center) Inhibition profiles of CC0651 analog titration on ubiquitination of phospho-Sic1 by SCF^{Cdc4} in vitro, as monitored by the addition of FAM-ubiquitin conjugates to phospho-Sic1. Data represented mean +/- S.E.M., n=2. (right) Effect of CC0651 analogs on Cdc34A-ubiquitin interaction by TR-FRET assay. Data represented as mean +/- S.E.M., n=2.

a

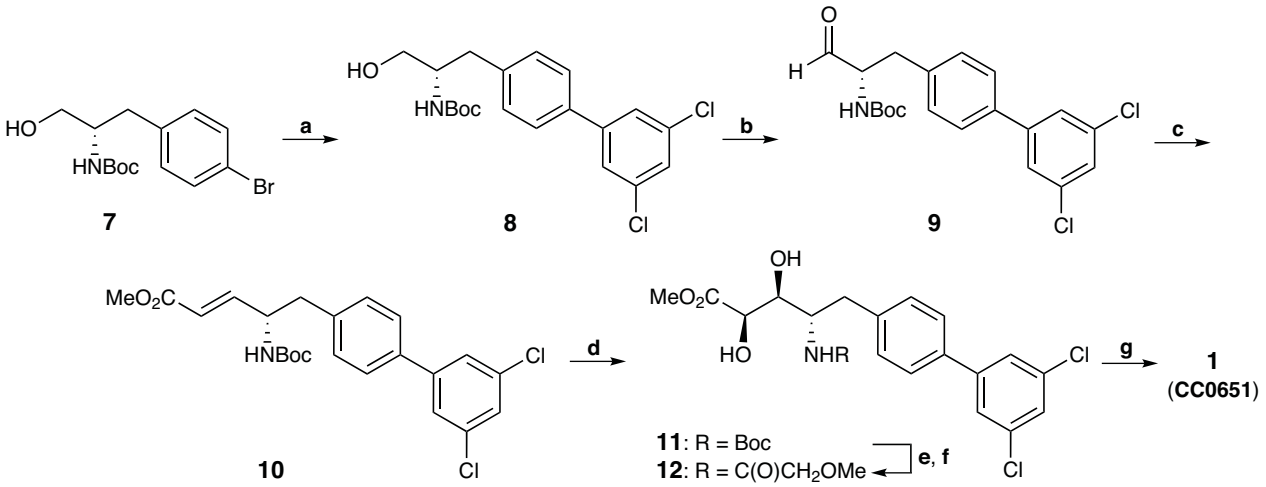

a. 3,5-$Cl_2C_6H_3B(OH)_2$, $Pd(PPh_3)_4$, Na_2CO_3, MeCN/H_2O (1:1), 80 °C, 93%; **b**. Dess-Martin reagent, CH_2Cl_2, 23 °C, 92%; **c**. $(MeO)_2P(O)CH_2CO_2Me$, DBU, LiCl, MeCN, 78%; **d**. $K_2OsO_2(OH)_4$, $(DHQ)_2Pyr$, $K_4Fe(CN)_4$, $MeSO_2NH_2$, K_2CO_3, $^tBuOH/H_2O$ (1:1), 54%; **e**. TFA, CH_2Cl_2; **f**. HO_2CCH_2OMe, HATU, DIPEA, MeCN, 81 % (for two steps); **g**. LiOH, THF, H_2O, 5 °C; then HCl 1 N, 5 °C, 63%.

b

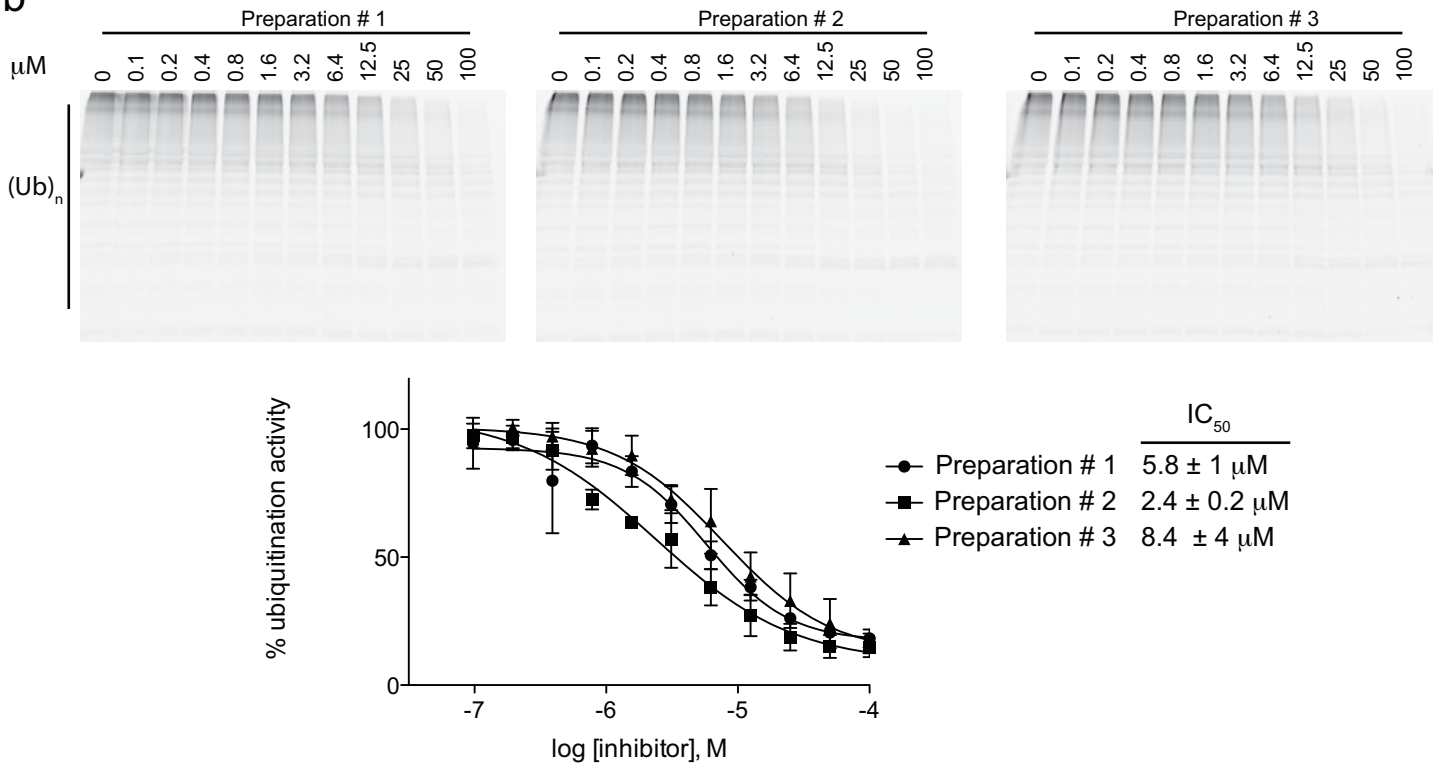

Supplementary Figure 12. Synthetic route for CC0651, and reproducibility of potency in vitro. (a) CC0651 synthesis. Chiral amino alcohol **7** and (3,5-dichlorophenyl)boronic acid substrates were subjected to a Suzuki cross-coupling reaction to afford biaryl intermediate **8**, which was selectively oxidized under non-racemizing conditions furnishing aldehyde **9**. Wittig olefination gave an a,b-unsaturated ester **10** which was diastereoselectively syn-dihydroxylated by Sharpless oxidation to give **11**. Boc deprotection followed by HATU-mediated acylation of the resulting amine with 2-methoxyacetic acid gave amide **12**. Saponification of **12** followed by acidification to pH 2 yielded CC0651. Chiral SFC analysis yielded an enantiomeric ratio of >98%. (b) Sensitivity of the SCF^{Cdc4} Sic1 ubiquitination reaction to different preparations of CC0651. Representative gels are shown for each preparation. IC_{50} values +/- S.E.M. were calculated for two replicate experiments.

Supplementary References

1. Reverter, D. & Lima, C. D. Insights into E3 ligase activity revealed by a SUMO-RanGAP1-Ubc9-Nup358 complex. *Nature* **435**, 687-692, (2005).
2. Hamilton, K. S. *et al.* Structure of a conjugating enzyme-ubiquitin thiolester intermediate reveals a novel role for the ubiquitin tail. *Structure* **9**, 897-904, (2001).
3. Spratt, D. E., Wu, K., Kovacev, J., Pan, Z. Q. & Shaw, G. S. Selective recruitment of an E2~ubiquitin complex by an E3 ubiquitin ligase. *J Biol Chem* **287**, 17374-17385, (2012).